Development of a thermally and chemically non-equilibrium model for decaying SF6 arc plasmas

Development of a Thermally and Chemically Non-Equilibrium Model for Decaying SF_6 Arc Plasmas

Yasunori Tanaka[1], Katsumi Suzuki[2], Takanori Iijima[3], Takeshi Shinkai[3]
[1] Kanazawa University, Kakuma, Kanazawa 920-1192, Japan
[2] Tokyo Denki University, Senjuasahi, Adachi-ku, 120-8551, Japan
[3] Toshiba Corporation, Ukishima, Kawasaki 210-0862, Japan

***Abstract*— This paper describes the development of a model with both chemically and thermally non-equilibrium effects in an SF_6 arc plasma during decaying phase with transient recovery voltage (TRV) application. The SF_6 arc plasma in decaying phase can be seen in a high voltage SF_6 gas circuit breaker during a large current interruption process. The TRV is often applied to the arc plasma, which may elevate the electron temperature T_e than heavy particle temperature T_h. This developed model solves energy equations for electrons and heavy particles, accounting for totally 122 reactions due to 19 species in SF_6 arc plasmas. As a result, transient distributions of T_e and T_h were calculated for SF_6 arc plasma in a TRV application condition for a fundamental study.**

I. Introduction

In a high-voltage gas circuit breaker, an SF_6 arc plasma is established between the electrodes during a high current interruption. This SF_6 arc is extinguished at current zero of the interrupting ac current by blowing SF_6 gas to the arc, which results in the current interruption in case of successful interruption. To downsize such a circuit breaker and to enhance its reliability, it is necessary to understand in detail arc interruption phenomena in SF_6 gas. One powerful tool for this purpose is numerical modeling of decaying SF_6 arcs. In conventional numerical models, local thermodynamic equilibrium (LTE) condition is often assumed to be established even in such decaying arcs. The LTE model assumes that all reactions have infinite reaction rates, and the all temperature are the same. However, in a transient state in a circuit breaker, the LTE assumption is not always established because some reactions requires finite time to reach their chemical equilibrium conditions. The chemically non-equilibrium model has been adopted for SF_6 thermal plasmas in [1]–[8]. We have developed a self-consistent chemically non-equilibrium model for decaying arc plasmas, and found that consideration of chemically non-equilibrium effects were important to determine the particle composition especially around the fringe of the arc plasma [9]–[11].

Another important non-equilibrium effects is due to thermally non-equilibrium condition. After the current zero, transient recovery voltage (TRV) is applied to the arc plasmas. Application of TRV to the arc may raise the electron temperature T_e more rapidly than heavy particle temperature T_h, i.e. gas temperature. For these cases, it is thus necessary to consider thermally non-equilibrium effects. Some researchers developed the two-temperature SF_6 model [4]–[8],[12]. However, a self-consistent chemically and thermally non-equilibrium model was not yet used accounting for reaction heat, thermodynamic and transport properties.

This paper focuses on modeling decaying SF_6 arcs with consideration of not only chemically non-equilibrium but also thermally non-equilibrium effects. One essential contribution of this paper is to indicate importance of considering these both non-equilibrium effects in decaying SF_6 arcs with TRV application. First, details of a developed model with both chemically and thermally non-equilibrium effects is interpreted. Finally, transient distribution of T_e and T_h, and chemical reaction fields were calculated for SF_6 arcs under a recovery state after simple voltage application. Results indicated that $T_e > T_h$ could be present in a residual SF_6 arc.

II. Modeling of SF_6 arc plasmas

The developed model assumes the following things in the SF_6 arc plasma for simplicity: (i) Axisymmetric structure, (ii) Laminar flow, (iii) Optically thin, (iv) Electron emission phenomena were not considered. (v) Evaporation of the electrode and the nozzle was neglected. (vi) 19 species SF_6, SF_5, SF_4, SF_3, SF_2, SF, S_2, F_2, S, F, SF^+, S_2^+, F_2^+, SF^-, S^+, F^+, S^-, F^-, e^- were taken into account as constituents in SF_6 arc plasmas. (vii) The electron temperature T_e can be different from the heavy-particle temperature T_h. (viii) Electrons, ions, and neutral particles have the same flow velocity. This allows a one-fluid model to be adopted.

A. Governing equations

On the assumptions of the previous section, the behavior of SF_6 arc plasmas is considered to be governed by the following equations. The most important point is that we consider both chemically and thermally non-equilibrium effects: Mass:

$$\frac{D\rho}{Dt} = -\rho(\nabla \cdot \boldsymbol{u}), \tag{1}$$

Momentum:

$$\rho\frac{D\boldsymbol{u}}{Dt} = -\nabla p + \nabla\cdot\boldsymbol{\tau}, \tag{2}$$

$$\boldsymbol{\tau} = \tau_{ij} = 2\eta\left[e_{ij} - \frac{1}{3}\delta_{ij}(\nabla\cdot\boldsymbol{u})\right] \tag{3}$$

Energy for heavy particles:

$$\begin{aligned}\rho_{\rm h}C_{\rm vh}\frac{DT_{\rm h}}{Dt} &= -p_{\rm h}(\nabla\cdot\boldsymbol{u}) + \nabla\cdot\left(\lambda^{\rm h}_{\rm tr}\nabla T_{\rm h}\right)\\ &\quad + Q_{\rm e-h} + Q^{\rm h}_{\rm heat}\end{aligned} \tag{4}$$

$$Q^{\rm h}_{\rm heat} = \sum_{j=1(j\neq {\rm e})}^{N}\nabla\cdot(\rho D_j h_j\nabla Y_j) + \sum_{\ell=1(\beta^{\rm f}_{{\rm e}\ell}\cdot\beta^{\rm r}_{{\rm e}\ell}=0)}^{L}\Delta Q_\ell \tag{5}$$

Energy for electrons:

$$\frac{3}{2}kn_{\rm e}\frac{DT_{\rm e}}{Dt} = \nabla\cdot(\lambda^{\rm e}_{\rm tr}\nabla T_{\rm e}) - Q_{\rm e-h} + Q^{\rm e}_{\rm heat} \tag{6}$$

$$\begin{aligned}Q^{\rm e}_{\rm heat} &= \nabla\cdot(\frac{1}{m_{\rm e}}\frac{5}{2}kT_{\rm e}\boldsymbol{\Gamma}_{\rm e}) + \sum_{\ell=1(\beta^{\rm f}_{{\rm e}\ell}\cdot\beta^{\rm r}_{{\rm e}\ell}\neq 0)}^{L}\Delta Q_\ell\\ &\quad + \sigma_{\rm e}|E|^2 - P_{\rm rad} - Q^{\rm e}_{\rm exc}\end{aligned} \tag{7}$$

Mass of species j:

$$\rho\frac{DY_j}{Dt} = \nabla\cdot(\rho D_j\nabla Y_j) + S_j, \tag{8}$$

$$S_j = m_j\sum_{\ell}^{L}(\beta^{\rm r}_{j\ell} - \beta^{\rm f}_{j\ell})\left(k^{\rm f}_\ell\prod_{i=1}^{N}n_i^{\beta^{\rm f}_{i\ell}} - k^{\rm r}_\ell\prod_{i=1}^{N}n_i^{\beta^{\rm r}_{i\ell}}\right) \tag{9}$$

The equation of state:

$$p = p_{\rm e} + p_{\rm h} \tag{10}$$

$$p_{\rm e} = n_{\rm e}kT_{\rm e} \tag{11}$$

$$p_{\rm h} = \sum_{j(j\neq {\rm e})}^{N}n_j kT_{\rm h} \tag{12}$$

Mass density:

$$\rho = \frac{p}{k\frac{Y_{\rm e}}{m_{\rm e}} + k\sum_{j=1(j\neq {\rm e})}^{N}\frac{Y_j}{m_j}T_{\rm h}} \tag{13}$$

Energy conversion by excitation:

$$\begin{aligned}Q^{\rm e}_{\rm exc} &= \sum_{j=1(j\neq {\rm e})}^{N}\left[k(T^j_{\rm ex})^2\frac{\partial\ln Z_j(T^j_{\rm ex})}{\partial T^j_{\rm ex}}\right.\\ &\quad \left. - kT_{\rm h}^2\frac{\partial\ln Z_j(T_{\rm h})}{\partial T_{\rm h}}\right]\nu_{\rm eh}n_{\rm e}\end{aligned} \tag{14}$$

Energy conversion by elastic collision:

$$Q_{\rm e-h} = \sum_{j=1(j\neq {\rm e})}^{N}\frac{3}{2}k(T_{\rm e} - T_{\rm h})\frac{2m_j m_{\rm e}}{(m_j + m_{\rm e})^2}\nu_{\rm eh}n_{\rm e} \tag{15}$$

Effective reaction heat:

$$\Delta Q_\ell = E_{{\rm reac}\ell}\left(k^{\rm f}_\ell\prod_{i=1}^{N}n_i^{\beta^{\rm f}_{i\ell}} - k^{\rm r}_\ell\prod_{i=1}^{N}n_i^{\beta^{\rm r}_{i\ell}}\right) \tag{16}$$

where ρ: mass density, t: time, $\boldsymbol{u}$: gas flow vector, p: pressure, $\boldsymbol{\tau}$: stress tensor, η: viscosity, e_{ij}: unit tensor, δ_{ij}: Kronecker delta, T: temperature, $C_{\rm vh}$: effective specific heat at constant volume for heavy particles, $\lambda_{\rm tr}$: translational thermal conductivity, D_j: effective diffusion coefficient, h_j: enthalpy of species j, Y_j: mass fraction of species j, $P_{\rm rad}$: radiation power, ΔQ_ℓ: heating power from reaction heat of reaction ℓ, m_j: mass of species j, $\beta_{j\ell}$: stoichiometric coefficient of species j for reaction ℓ, $k^{\rm f,r}_\ell$: reaction rate coefficient for reaction ℓ, n_j: density of species j, $\nu_{\rm eh}$: collision frequency between the electron and heavy particles, $E_{{\rm reac}\ell}$: Reaction heat for reaction ℓ, k: Boltzmann constant, $\frac{D}{Dt} = \frac{\partial}{\partial t} + \boldsymbol{u}\cdot\nabla$ is the Lagrangian derivative.

Solving (8) enables calculation of particle composition in the SF_6 arc plasma considering chemically non-equilibrium effects. On the other hand, solving the energy equations for electrons and heavy particles allows us to derive the $T_{\rm e}$ and $T_{\rm h}$ from thermally non-equilibrium effects. In Eqs.(4) and (6), the energy conversions between the electron and heavy particles were taken into account to couple both energy conservations. In Eq.(6), we accounted equivalently for the energy conversion by excitation reaction through electron impact processes, using the effective excitation temperature $T^j_{\rm ex}$ for species j [13]. The $T^j_{\rm ex}$ was also used for calculation of h_j and $C_{\rm Vh}$ to take into account the effect of electronic excitation of species j.

B. Properties and rate coefficients for reactions

The thermodynamic and transport properties are necessary for fluid dynamics simulation such as specific heat $C_{\rm vh}$, enthalpy h_j, translational thermal conductivity for heavy particles $\lambda^{\rm h}_{\rm tr}$, translational thermal conductivity for electrons $\lambda^{\rm e}_{\rm tr}$, viscosity η, $P_{\rm rad}$. These properties should be self-consistently calculated using the computed particle composition, both $T_{\rm e}$ and $T_{\rm h}$, and the collision integrals at each position at each calculation step. This self-consistent calculation was done in the present model. The calculation of the transport properties were based on the first order approximation of Chapman-Enskog method.

For consideration of chemically non-equilibrium effects, the developed model accounted for 61 reactions including the electron impact ionization, the electron attachment, the electron impact dissociation, other chemical reactions, and their backward reactions [9]. Temperature dependent rate coefficients for these reactions were obtained in literatures [4]−[8]. Rate coefficients for their backward reactions were calculated through the principle of detailed balance. Reaction rate coefficient was assumed to depend on $T_{\rm e}$ when the electron is included as reactants, otherwise it depends on $T_{\rm h}$.

C. Calculation space and boundary condition

Fig. 1 illustrates the calculation space in this paper. This space was divided by 153×170 grids for the r-z two-dimensional calculation space. Boundary conditions were set as follows: The nozzle and the electrode has a non-slip wall with condition u=v=0. At the axis, v and the radial derivatives of physical parameters of u, $T_{\rm e}$, $T_{\rm h}$, p and ρ were set to zero. At the inlet around z=0 mm, the

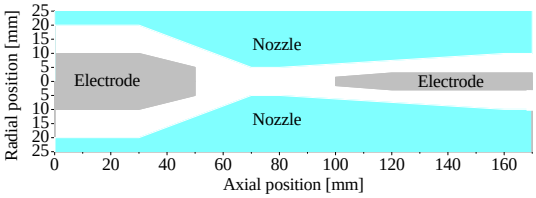

Fig. 1. Calculation domain.

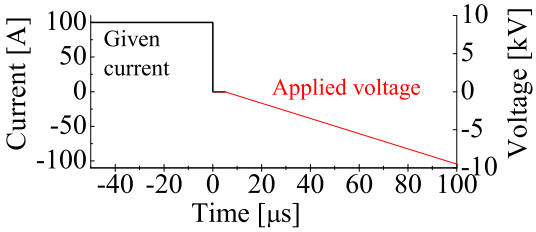

Fig. 2. Current and applied voltage given in the calculation.

gas flow and the temperature were set 10 m/s and 300 K, respectively. At the outlet, the axial derivatives of the parameters were set to zero. The pressure at one point of the outlet was fixed at 0.5 MPa. This calculation neglected evaporation of the nozzle and the electrode for simplicity.

In this calculation, the following electrical circuit condition was imposed to the arc plasma. Fig. 2 shows the current and applied voltage given. First, the steady state calculation was made for a current of dc 100 A. In this calculation, the current was given and the arc voltage was computed. For steady state calculation, the SIMPLE algorithm was used. Then, the transient state calculation was made for a current stepped down from 100 A to 0 A. From 5μs after current down from 100 A to 0 A, the transient recovery voltage (TRV) was applied with a rise of rate of recovery voltage (RRRV). The reason why a 5 μs delay was set before TRV application is that TRV application without a delay causes the large current, and then failure of current interruption. The value of RRRV for this paper is 0.1 kV/μs. For transient calculation, the C-CUP algorithm was adopted.

III. Results

A. Transient distribution of electron temperature and heavy particle temperature

Figs. 3–6 depict the temperature distributions between the electrodes in an SF_6 arc at t = 0, 2, 10, and 50 μs after current zero. The upper panels in these figures are the temperature T calculated by a one-temperature chemically non-equilibrium (1T-NonCE) model that we have previously developed [9]. These are shown for comparison. The middle and lower panels are respectively T_h and T_e calculated by the two-temperature chemically non-equilibrium (2T-NonCE) model developed in the present paper. The TRV was applied from t = 5 μs after current zero. Fig. 3 corresponds to the results at t = 0 μs, i.e. for steady state calculation results for 100 A. This is the initial condition with T=T_h=T_e.

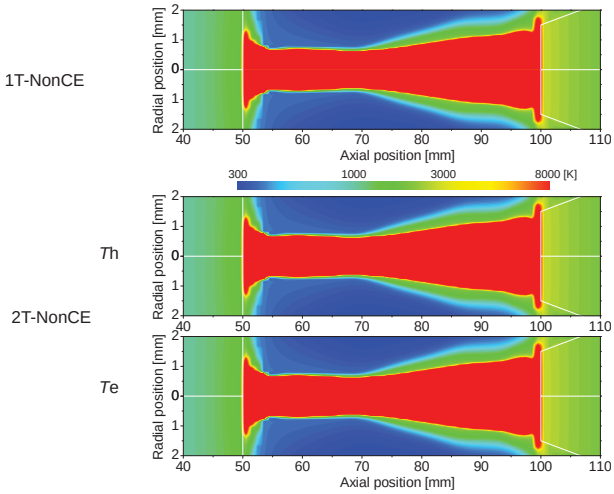

Fig. 3. Temperature distributions between the electrodes in an SF_6 arc at t = 0 μs after current zero. The upper panel is the temperature calculated by the one-temperature chemically non-equilibrium (1T-NonCE) model, the middle and the lower panels are respectively the heavy particle temperature T_h and the electron temperature T_e calculated by the two-temperature chemically non-equilibrium (2T-NonCE) model.

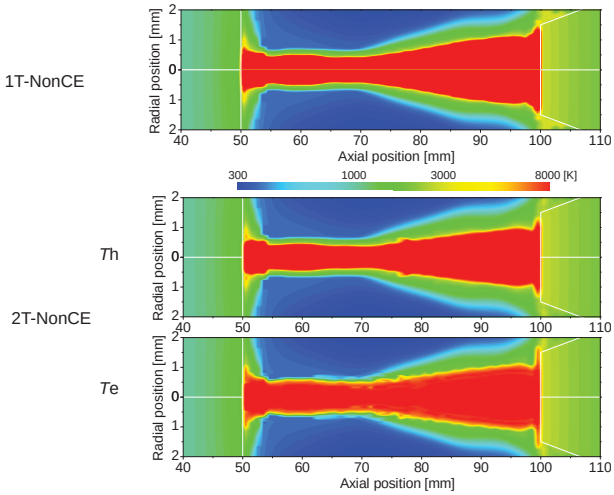

Fig. 4. Temperature distributions between the electrodes in an SF_6 arc at t = 2 μs after current zero. The upper panel is the temperature calculated by the one-temperature chemically non-equilibrium (1T-NonCE) model, the middle and the lower panels are respectively the heavy particle temperature T_h and the electron temperature T_e calculated by the two-temperature chemically non-equilibrium (2T-NonCE) model.

First, we noticed a difference between T_e and T_h. After current down from 100 A to 0 A at t = 0 μs, the arc temperature decays rapidly with time. At t = 2 μs after current zero without TRV application yet, both T_h and T_e decreases with time, almost with a similar decaying rate. On the other hand, at t = 10 μs after current zero, there is a big difference between T_e and T_h. At this instance, applied voltage reaches to 0.5 kV. As seen in Fig. 5, a region $T_e > T_h$ clearly exists in the decaying arc. This is attributed to the fact that TRV application accelerates the electrons in the arc plasma, effectively resulting in higher T_e than T_h compared to the energy relaxation process from electrons to heavy particles. At t = 50 μs after current zero with an applied voltage

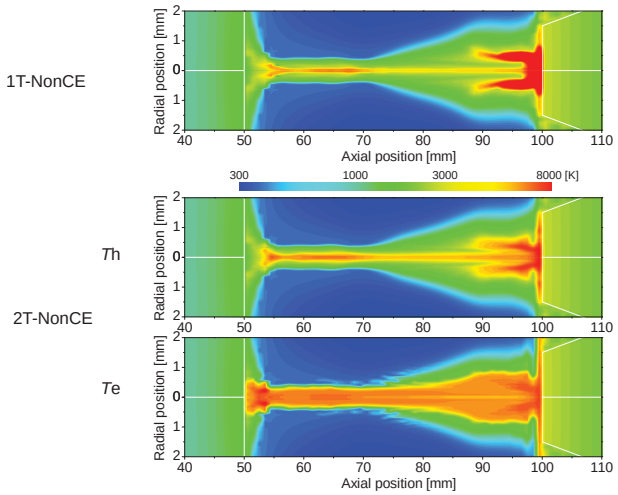

Fig. 5. Temperature distributions between the electrodes in an SF_6 arc at t = 10 μs after current zero. The upper panel is the temperature calculated by the one-temperature chemically non-equilibrium (1T-NonCE) model, the middle and the lower panels are respectively the heavy particle temperature T_h and the electron temperature T_e calculated by the two-temperature chemically non-equilibrium (2T-NonCE) model.

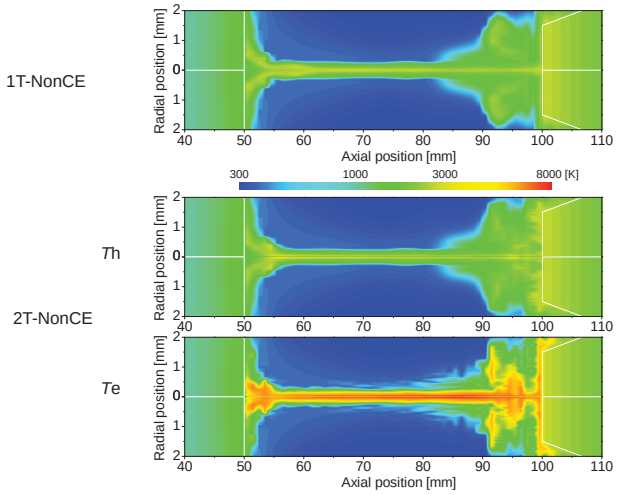

Fig. 6. Temperature distributions between the electrodes in an SF_6 arc at t = 50 μs after current zero. The upper panel is the temperature calculated by the one-temperature chemically non-equilibrium (1T-NonCE) model, the middle and the lower panels are respectively the heavy particle temperature T_h and the electron temperature T_e calculated by the two-temperature chemically non-equilibrium (2T-NonCE) model.

of 4.5 kV, a relationship $T_e > T_h$ is obviously found inside the residual arc plasma. This shows that thermally non-equilibrium effects should be taken into account in simulation of decaying SF_6 arc plasmas. Fig. 7 shows the time evolutions in T_e and T_h at nozzle throat inlet position z=70 mm on the axis after TRV application. The quantity T_h decreases with time in the decaying SF_6 arc, and T_e also declines from t = 5 to 27 μs with a lower decay rate than T_h. However, T_e increases with time from t = 27 μs, finally reaching to 6217 K at t = 55 μs. This value is 3400 K higher than T_h.

Next, attention was paid to a difference between the temperature T by the 1T-NonCE model, and T_h by the 2T-NonCE model. The one-temperature model only solves

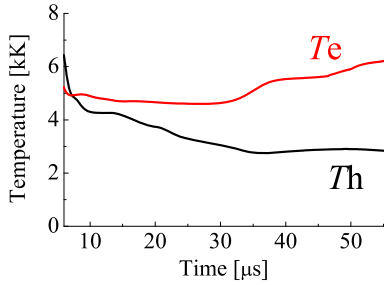

Fig. 7. Time evolution in electron temperature and heavy particle temperature at nozzle throat inlet in an SF_6 arc after application of transient recovery voltage.

one energy conservation equation for electrons and heavy particles to obtain arc temperature T. As seen in Figs. 3–6, the T by 1T-NonCE model has rather a similar value to the T_h by 2T-NonCE model from t = 0 μs to 50 μs. This signifies that one-temperature model only simulates the behavior of T_h, and it cannot express the T_e behavior. The behavior of T_e is crucial to determine the electron impact reactions like ionization and dissociation after TRV application.

IV. Summary

A two-dimensional numerical thermo-fluid model of SF_6 arc plasmas was developed with consideration of not only chemically non-equilibrium effects but also thermally non-equilibrium effects self-consistently. This was developed because the transient recovery voltage (TRV) is applied to the electrodes in a circuit breaker after current interruption, and it may be possible to involve a two-temperature condition in a residual arc plasmas. The developed model considers 19 species and 122 reactions in SF_6 arc plasmas for consideration of chemically non-equilibrium effects. Two energy equations for electrons and heavy particles were separately solved to obtain the behaviors of electron temperature T_e and heavy particle temperature T_h. Results showed that region $T_e > T_h$ was clearly present in a residual SF_6 arc plasma in case of TRV application with RRRV=0.1 kV/μs. These results suggest that thermally non-equilibrium effects should be considered in a circuit breaker arc model.

References

[1] Y.Tanaka, et al., *Proc. 12th Int. Conf. Gas Discharges & Their Appl.*, Vol.II, pp.566–569, 1997.9.
[2] Y.Tanaka, et al., *Proc. Int. Conf. on Electr. Eng. ICEE'98*, pp.583–586, 1998.7.
[3] Y.Tanaka and T.Sakuta, *Proc. 14-th Int. Symp. on Plasma Chem. ISPC-14*, pp.245–250, 1999.8.
[4] R.Girard, et al., *J.Phys.D:Appl.Phys.*, **32**, 1229–1238, 1999.
[5] A.Gleizes, et al., *J. Phys. D: Appl. Phys.*, **32**, 2060–2067, 1999.
[6] R.Girard, et al., *J. Phys. D: Appl. Phys.*, **32**, 2890–2901, 1999.
[7] I.Coll, et al., *J. Phys. D: Appl. Phys.*, **33**, 221–229, 2000.
[8] J.J.Gonzalez, et al., *J. Phys. D: Appl. Phys.*, **33**, 2759–2768, 2000.
[9] Y.Tanaka, K.Suzuki, *Proc. the First Int. Conf. Electric Power Equip. Switching Technol., ICEPE2011*, pp.492–495, 2011.
[10] Y.Tanaka, T.Shinkai, *Int.Conf. Electr. Eng., ICEE2012*, P-PS1-1 , 2012.
[11] Y.Tanaka, T.Shinkai, *Proc. 19th Int.Conf. Gas Discharges & their Appl., GD2012*, pp.66–69, 2012.
[12] W.Z.Wang, et al., *J. Phys. D: Appl. Phys.*, **46**, 065203, 2013.
[13] Y. Tanaka, et al., *IEEE Trans. Plasma Sci.*, **25**, 991–995, 1997.